The Ternary System (*n*-Heptane + Docosane + Tetracosane): The Solubility of Mixtures of Docosane and Tetracosane in Heptane and Data on Solid−Liquid and Solid−Solid Equilibria in the Binary Subsystem (Docosane + Tetracosane)

Eckhard Flöter, Bart Hollanders, Theodoor W. de Loos,* and Jakob de Swaan Arons

Delft University of Technology, Department of Chemical Engineering and Materials Science, Laboratory of Applied Thermodynamics and Phase Equilibria, Julianalaan 136, 2628 BL Delft, The Netherlands

In this paper experimental data on the solid−liquid and solid−solid equilibria in the binary system (docosane + tetracosane) and solid solubility data in the ternary system (heptane + docosane + tetracosane) are presented. For 14 binary mixtures of the two heavy alkanes, DSC measurements were performed to detect the solid−liquid and solid−solid phase transition temperatures. Solid disappearance temperatures were measured for 14 mixtures of docosane and tetracosane dissolved in various quantities of heptane. The experimental results reveal that the solubility curves found in the ternary system correspond to the phase behavior of the binary subsystem studied. At low concentrations of heptane, probably almost ideally mixed crystals are in equilibrium with the liquid phase, while at high heptane concentrations, the solid−liquid equilibrium involves most likely different nonideal solid phases.

Introduction

The controlled precipitation of solid phases from multicomponent fluid mixtures is widely applied in, e.g., chemical, pharmaceutical, and food industries as a separation method. However, in the petroleum industry it is an undesirable phenomenon (wax formation) which severly hampers transportation or other processes taking place (Erickson et al., 1993; Reddy, 1986; Keating and Wattenberger, 1994). No matter whether one wants to control or prevent the precipitation of either mixed or pure solid phases from solutions, adequate thermodynamical models should be available to describe the phase behavior of the system under consideration.

In the past, the wax formation problem was mainly handled on the basis of empirical models. In recent years, more effort has been spent on the development of adequate thermodynamical models (Coutinho, 1995; Lira-Galeana et al., 1996). A general problem faced is the scarcity of experimental data on the phase behavior of well-defined multicomponent mixtures. Abundant experimental data are available on systems with either only one solute (Kniaź, 1991) or two solutes certainly precipitating as independent pure component crystals (Jakob et al., 1995). Further experimental data sets are available on binary systems possibly forming mixed crystals, which means the absence of a solvent (Mazee, 1960; Sabour et al., 1995; Achour et al., 1992; Dorset, 1990; Maroncelli et al., 1985). Other data sets on real reservoir fluids or fuels (Holder and Winkler, 1965; Van Winkle et al., 1987) do not allow us to make a clear distinction between different mechanisms involved in the solid precipitation, due to characterization procedures and experimental accuracies (Erickson et al., 1993).

To bridge the gap between the different type of data sets available in the literature, it is desirable to have phase equilibrium data for systems of one solvent and a few solutes that are known to form mixed crystals in at least one of the binary subsystems. Some data sets are available for these kinds of systems (Ghogomu et al., 1989; Roberts et al., 1994; Asbach and Kilian, 1991). In this paper, experimental results on the solid solubility in the ternary system composed of *n*-heptane, docosane, and tetracosane for 14 relative solute concentrations are presented. Additionally, experimental data on the phase behavior of 14 mixtures of docosane and tetracosane are presented.

* Corresponding author.

Experimental Section

The chemicals used in this study were tetracosane supplied by Janssen Chimica with a stated purity of better than 99 mass %, docosane supplied by Aldrich with a stated purity of better than 99 mass %, and *n*-heptane supplied by Fluka with a stated purity better than 99.5 mass %. DSC analyses of the docosane and the tetracosane showed less than 0.5 mole % impurities, respectively, which were not further identified. All chemicals were used without further purification.

The experiments on the binary subsystem (docosane + tetracosane) were carried out with a differential scanning calorimeter (DSC Polymer Laboratories, Gold-Cell). The calibration of the calorimeter was based on the melting temperatures of pure gallium and pure indium. Binary samples of about 5 mg weight were prepared by weight using a Sartorius microbalance (Type M3P). This results in an accuracy of better than ±0.005 in mole fraction for the composition of the sample.

The applied heating rates were 2 K min^{-1}. To determine the different transition temperatures from the DSC curves, the following procedure was applied. For a monovariant transition the corrected onset temperature was equated with the transition temperature. In cases of a nonisothermal solid−solid or solid−liquid transition, the lower transition temperature was again equated with the corrected onset temperature. The higher temperature of the transition interval was, following a reasoning given elsewhere (Schawe, 1993; Höhne et al., 1994; Asbach et al., 1982), equated with the point of inflection in the rising flank of the peak. The accuracy of the monovariant phase transition temperature determined is ±0.25 K. For the nonisothermal transitions of the binary mixtures, the accuracies of the solidus α, solidus β, and liquidus temperatures are better than ±0.5 K.

S0021-9568(96)00332-9 CCC: $14.00

Table 1. Temperatures of Phase Transitions in the System (Docosane (A) + Tetracosane (B)): $T_{SS\ low}$ (s^β or $s^\gamma \rightarrow s^\beta$ or $s^\gamma + s^\alpha$); $T_{SS\ high}$ (s^β or $s^\gamma + s^\alpha \rightarrow s^\alpha$); $T_{SL\ low}$ ($s^\alpha \rightarrow s^\alpha$ + Liquid); $T_{SL\ high}$ (s^α + Liquid → Liquid)

x_B	$T_{SS\ low}$/K	$T_{SS\ high}$/K	$T_{SL\ low}$/K	$T_{SL\ high}$/K
0.000	315.56	315.56	317.06	317.06
0.036	305.00	305.35	316.90	317.44
0.079	302.79	303.20	317.11	317.78
0.148	301.90	302.24	317.47	318.31
0.219	301.60	302.03	317.56	318.87
0.270	301.28	301.73	317.64	319.03
0.363	301.75	302.66	318.55	319.73
0.503	303.15	304.56	319.26	320.38
0.609	304.75	306.61	320.22	321.52
0.709	307.32	308.81	320.95	322.04
0.796	309.16	311.04	321.40	322.95
0.859	311.47	312.57	322.08	323.15
0.930	315.79	316.78	322.50	323.43
1.000	320.39	320.39	323.44	323.44

The experiments on the solid solubility in the ternary system were based on the visual observation of the disappearance of the solid phase with increasing temperature. The samples are again prepared on a weight basis. The total amount of the two solutes contained in a glass sample tube is for all mixtures approximately 1 g. Via a septum in the lid of the sample tube, subsequently, distinct amounts of *n*-heptane were added to the sample from a syringe. The amount of *n*-heptane added is again determined on a weight basis. Due to the procedure applied, the accuracy of the composition deteriorates in the course of an experimental run. However, the uncertainty does not exceed ±0.01 in the mole fraction of *n*-heptane, while the accuracy of the relative mole fraction of the two solutes is better than ±0.005.

The different sample tubes are placed in a thermostated water bath (Lauda Type CSG) controlled within ±0.03 K. Mixing and temperature equilibrium are established by agitation of a stirrer inside the tube by magnetic coupling. Temperatures are measured by means of a Pt-100 resistance thermometer connected to a resistance bridge (ASL F-16). The accuracy of the temperature measurement is ±0.01 K.

Through storage at lower temperatures, the samples are brought into a two-phase (solid + liquid) state. After the samples are placed in the thermostated water bath, the temperature is gradually increased until the disappearance of the solid phase is visually detected. This procedure is repeated several times, so that for a given composition the solution temperature is determined to an accuracy better than ±0.25 K.

Results

The experimental results of the differential scanning calorimetry are given in Table 1. In Figure 1 the experimental results on solid−liquid and solid−solid equilibria are displayed. For comparison also the transition and melting temperatures given in literature (Mazee, 1960; Achour et al., 1992) are included. Regarding the scattering of the literature data, it seems fair to conclude that the literature data and our data agree and that the data presented here increase the certainty of the course of the phase boundaries found in the system {docosane (A) + tetracosane (B)}. This holds especially for the melting behavior of mixtures containing mainly docosane. For these mixtures both literature sources give solidus temperatures lower than the melting point temperature of pure docosane. This is, excluding the presence of other solid phases, only possible in a so-called hylotrope where as in an azeotrope, the coexisting phases are of equal composition. The data given in the literature do not indicate this kind of compositional behavior. For the solid−solid transition a distinct temperature minimum with $T = 301.4$ K at a tetracosane mole fraction of 0.24 is found. Further, two discontinuities in the solid−solid phase boundaries are found for mixtures with a mole fraction of tetracosane of approximately 0.05 and 0.85.

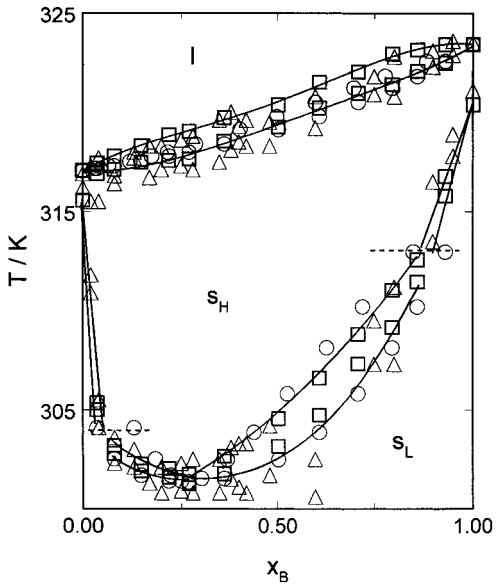

Figure 1. Solid−solid and solid−liquid phase transition boundaries in the binary system (docosane (A) + tetracosane (B)). Key: (□) this work; (△) Achour et al. (1992); (○) Mazee (1960); s_L, low-temperature solid form with either triclinic or orthorhombic structure; s_H, high-temperature solid form with hexagonal structure; l, liquid phase. Lines were drawn to guide the eye.

Solid solubilities in the ternary system {heptane (C) + docosane (A) + tetracosane (B)} are determined for 14 different mole fraction ratios of docosane and tetracosane. Table 2 contains the experimental solid disappearance temperatures as a function of the heptane mole fraction. Our results on the solid solubilities in the binary subsystems incorporating heptane agree quite well with the data given in the literature (Roberts et al., 1994; Domańska and Rolińska, 1989; Brečević and Garside, 1993; Domańska, 1996). No literature data are available on the solubilities in the ternary system studied. Figure 2 shows the solid disappearance temperatures for different ratios of tetracosane and docosane at a fixed heptane mole fraction of 0.75. Following the interpretation of Coutinho (1995), the proposed discontinuities in the line drawn to guide the eye separate the regions of different solid structures. In Figure 3 isothermal solid solubility curves are displayed. For higher temperatures the solid solubility curves connect the two binary subsystems almost linearly. With the increasing mole fraction of heptane this changes. At lower temperatures the solubility is significantly increased compared to a hypothetical ideal solid solution—as is easily derived, the isothermal solubility curve in a system with ideal mixtures in the liquid and solid phases is curved toward higher heptane concentrations. Close to the binary subsystem (heptane + docosane) a maximum of solubility is detected for the different isotherms.

Discussion

The experimental results on the phase behavior of the binary system {docosane (A) + tetracosane (B)} are in good agreement with literature data (Achour et al., 1992; Mazee, 1960). However, our data are more consistent since the scattering is much smaller than for the literature data. The

Table 2. Solubility of Mixtures of (Docosane (A) + Tetracosane (B)) in Heptane (C) as a Funtion of Heptane Mole Fraction x_C for Fixed $x_B^* = n_B/(n_A + n_B)$

x_C	T/K	x_C	T/K	x_C	T/K	x_C	T/K	x_C	T/K
$x_B^* = 0$		$x_B^* = 0.162$		$x_B^* = 0.411$		$x_B^* = 0.607$		$x_B^* = 0.823$	
0.000	317.55	0.000	318.70	0.000	321.36	0.000	321.97	0.000	322.65
0.260	313.41	0.325	311.34	0.118	318.28	0.255	317.15	0.256	319.18
0.504	309.15	0.541	305.54	0.299	314.58	0.489	311.37	0.505	313.78
0.752	300.00	0.750	296.65	0.611	305.54	0.740	301.95	0.752	305.40
0.900	291.54	0.902	287.60	0.747	300.36	0.894	293.29	0.901	297.11
0.951	284.29	0.950	279.76	0.895	290.30	0.946	285.49	0.950	288.38
$x_B^* = 0.063$		$x_B^* = 0.273$		$x_B^* = 0.545$		$x_B^* = 0.665$		$x_B^* = 1.000$	
0.000	316.80	0.000	319.01	0.000	320.31	0.000	322.40	0.000	323.78
0.473	307.02	0.214	315.27	0.192	317.75	0.195	319.50	0.273	319.51
0.638	302.50	0.310	313.69	0.353	315.42	0.317	317.17	0.512	316.03
0.793	294.62	0.545	306.83	0.433	312.87	0.494	312.18	0.754	308.32
0.908	286.73	0.599	304.99	0.606	307.44	0.606	307.55	0.901	299.15
0.954	283.25	0.775	297.49	0.757	301.54	0.769	304.50	0.950	289.47
		0.905	287.86	0.912	291.75	0.904	295.56		
$x_B^* = 0.156$		0.953	281.15	0.953	285.13	0.950	289.45		
0.000	317.35								
0.179	314.37	$x_B^* = 0.375$		$x_B^* = 0.604$		$x_B^* = 0.709$			
0.337	311.23	0.000	319.25	0.000	321.45	0.000	322.15		
0.491	307.25	0.273	315.41	0.253	317.55	0.200	319.35		
0.602	303.42	0.501	309.57	0.589	308.35	0.509	311.55		
0.760	297.04	0.750	298.75	0.765	301.65	0.755	303.45		
0.909	286.47	0.900	288.61	0.902	292.05	0.901	295.55		
0.954	279.66	0.950	281.68	0.952	285.35	0.952	289.45		

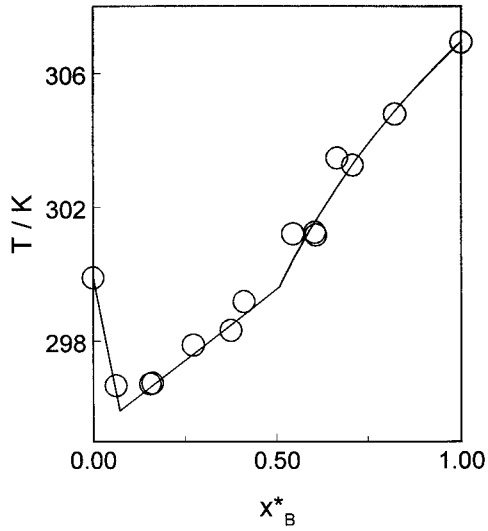

Figure 2. Solid disappearance temperatures for mixtures of (docosane (A) + tetracosane (B)) in heptane (C) at constant heptane mole fraction $x_C = 0.75$. Temperature versus relative solute mole fraction $x_B^* = n_B/(n_A + n_B)$.

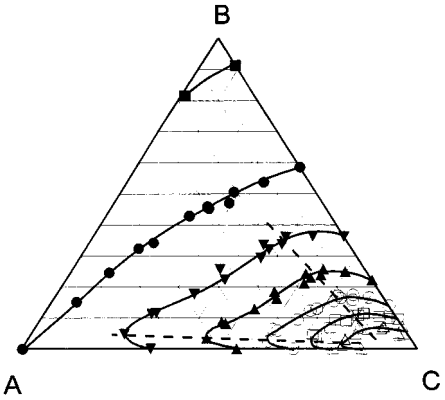

Figure 3. Isothermal solubility curves in the ternary system (heptane (C) + docosane (A) + tetracosane (B)). From right to left: (△) 294.1 K; (□) 298.5 K; (○) 303.0 K; (▲) 307.7 K; (▼) 312.5 K; (●) 317.5 K; (■) 322.5 K. Dashed lines indicate discontinuities as shown in Figure 2. Full lines were drawn to guide the eye.

smooth curves found clearly indicate that there is no temperature minimum present for the solid−liquid transition at high docosane concentrations. An extensive discussion of the different solid phases found below the solid−solid transition is given by Achour et al. (1992). Close to the pure components, regions of mixed crystals of triclinic structure are found, while in the intermediate composition range, three regions characterized by different orthorhombic structures are present (Achour et al., 1992). The discontinuities of the solid−solid transition curves found most likely correspond to the changes of the crystal structure from triclinic to orthorhombic.

In the ternary system {heptane (C) + docosane (A) + tetracosane (B)}, the shape of the solubility curves found, see Figures 2 and 3, show systematic patterns. For the correct interpretation of the experimental results, the phase behavior of the binary subsystem (docosane + tetracosane) is of major importance. From the experimental results it seems fair to conclude that the mixed crystal formed at higher temperatures (322.5 K, 317.5 K) is almost ideally mixed. Taking this and the information given elsewhere (Coutinho, 1995) into account, it is most likely that this mixed crystal is of hexagonal structure. At lower temperatures, or higher heptane concentrations, the solubility curves reveal discontinuities. These are shown in Figure 2 and indicated with dashed curves in Figure 3. Following the same reasoning as above, these discontinuities can be related to the appearance of the different solid structures. With increasing mole fraction of heptane x_C and decreasing temperature, the ternary solution is in equilibrium with a mixed solid phase with, depending on the relative solute concentration, either a triclinic, hexagonal, or orthorhombic structure. Similar results were found by Ghogomu et al. (1989) for the systems (ethylbenzene + docosane + tetracosane) and (ethylbenzene + tricosane + tetracosane). They also reported maxima of the isothermal solubility curves for high relative solute mole fractions of the shorter *n*-alkane.

Literature Cited

Achour, Z.; Barbillon, P.; Bouroukba, M.; Dirand, M. Determination of the phase diagram of the system docosane (n-C_{22})-tetracosane (n-C_{24}): variation of the enthalpy. *Thermochim. Acta* **1992**, *204*, 187−204 (in French).

Asbach, G. I.; Kilian, H. G. Investigation of Equilibrium Crystallization Processes of n-Alkane Multicomponent Systems. *Polymer* **1991**, *32*, 16, 3006−3012.

Asbach, G. I.; Kilian, H. G.; Stracke, Fr. Isobaric Binary State Diagrams of n-Alkanes. *Colloid Polym. Sci.* **1982**, *260*, 151−163.

Brečević, L.; Garside, J. Solubilities of Tetracosane in Hydrocarbon Solvents. *J. Chem. Eng. Data* **1993**, *38*, 598−601.

Coutinho, J. A. P. Phase Equilibria in Petroleum Fluids, Multiphase Regions and Wax Formation. Ph.D. thesis, Technical University of Denmark, Lyngby, 1995.

Domańska, U. Solubility of docosane in heptane. Private communication, 1996.

Domańska, U.; Rolińska, J. Correlation of the Solubilty of Even-Numbered Paraffins $C_{20}H_{42}$, $C_{24}H_{50}$, $C_{26}H_{54}$, $C_{28}H_{58}$ in Pure Hydrocarbons. *Fluid Phase Equilib.* **1989**, *45*, 25−38.

Dorset, D. L. Chain Length and the Cosolubilty of n-Paraffins in the Solid State. *Macromolecules* **1990**, *23*, 623−633.

Eriksson, D. D.; Niesen, V. G.; Brown, T. S. Thermodynamic Measurement and Prediction of Paraffin Precipitation in Crude Oil. SPE paper No. 26604. Presented at 68th annual SPE Technical conference, Houston, TX, Oct 3−6, 1993.

Ghogomu, P. M.; Dellacherie, J.; Balesdent, D. Solubility of Normal Paraffin Hydrocarbons (C_{20} to C_{24}) and some of their Binary Mixtures (C_{22} + C_{24}) and (C_{23} + C_{24}) in Ethylbenzene. *J. Chem. Thermodyn.* **1989**, *21*, 925−934.

Höhne, G. W. H.; Blankenhorn, K. High Pressure DSC Investigations on n-Alkanes, n-Alkane Mixtures and Polyethylene. *Thermochim. Acta* **1994**, *238*, 351−370.

Holder, G. A.; Winkler, J. Wax Crystallization from Distillate Fuels. Part I. Cloud Point and Pour Point Phenomena Exhibited by Solutions of Binary n-Paraffin Mixtures. *J. Inst. Petrol.* **1965**, *51*, 228−234.

Jakob, A.; Joh, R.; Rose, C.; Gmehling J. Solid-Liquid Equilibria in Binary Mixtures of Organic Compounds. *Fluid Phase Equilib.* **1995**, *113*, 117−126.

Keating, J. F.; Wattenberger, R. A. The Simulation of Paraffin Deposition and Removal from Wellbores. SPE paper No. 27871, 1994.

Kniaź, K. Influence of Size and Shape Effects on the Solubility of Hydrocarbons: the Role of the Combinatorial Entropy. *Fluid Phase Equilib.* **1991**, *68*, 35−46.

Lira-Galeana, C.; Firoozabadi, A.; Prausnitz, J. M. Thermodynamics of Wax Precipitation in Petroleum Mixtures. *AIChE J.* **1996**, *42*, 1, 239−248.

Maroncelli, M.; Strauss, H. L.; Snyder, R. G. Structure of the n-Alkane Binary Solid n-$C_{19}H_{40}$/n-$C_{21}H_{44}$ by Infrared Spectroscopy and Calorimetry. *J. Phys. Chem.* **1985**, *89*, 5260−5267.

Mazee, W. M. Paraffin, its composition and the phase behavior of its main components, the n-alkanes. *Erdoel Kohle* **1960**, *13*, 2, 88−93 (in German).

Reddy, S. R. A Thermodynamic Model for Predicting n-Paraffin Crystallization in Diesel Fuel. *Fuel* **1986**, *65*, 1647−1652.

Roberts, K. L.; Rousseau, R. W.; Teja, A. S. Solubility of Long Chain n-Alkanes in Heptane Between 285 and 350 K. *J. Chem. Eng. Data* **1994**, *39*, 793−795.

Sabour, A.; Bourdet, J. B.; Bouroukba, M.; Dirand, M. Modifications to the Phase Diagram of the n-Alkane Mixtures n-C_{23}-n-C_{24}. *Thermochim. Acta* **1995**, *249*, 269−283.

Schawe, J. E. K. A New Method to Estimate Transition Temperatures and Heats by Peak Form Analysis. *Thermochim. Acta* **1993**, *259*, 69−84.

Van Winkle, T. L.; Affens, W. A.; Beal, E. J.; Mushrush, G. W.; Hazlett, R. N.; DeGuzman, J. Distribution of n-Alkanes in Partially Frozen Middle Distillate Fuels. *Fuel* **1987**, *66*, 947.

Received for review October 23, 1996. Accepted February 10, 1997.[⊗]

JE960332C

[⊗] Abstract published in *Advance ACS Abstracts,* April 1, 1997.